Atomic Structure of Si(111)-(5 × 2)-Au from High Resolution Electron Microscopy and Heavy-Atom Holography

L. D. Marks and R. Plass

Department of Materials Science and Engineering, Northwestern University, Evanston, Illinois 60208

(Received 24 April 1995)

The main elements of the atomic structure of the Si(111)-(5 × 2)-Au surface have been found by combining off-zone high resolution electron microscopy with χ^2 electron diffraction minimization and direct phasing of the diffraction data using heavy-atom holography. The structure is different from recent models based upon interpreting scanning tunneling microscope and x-ray data in terms of disordered arrangements of gold atoms, and much simpler. It contains two lines of gold atoms decorating a surface dislocation plus an expanded surface arrangement of silicon atoms. This model appears to explain all the available experimental data and is consistent with an expansive surface stress for Si(111).

PACS numbers: 61.14.Rq, 61.10.My, 61.16.Bg, 68.35.Bs

One of the most fundamental questions in surface science and growth studies is the atomic structure of monolayers or submonolayers on a substrate. Despite several decades of study, many of these structures are still unclear. One example is the gold on silicon (111) surface in the coverage regime of 0.4–0.5 monolayer (ML), where a large amount of apparently conflicting information is available. From early LEED studies [1,2] the basic unit cell is 5 × 2, with phase slippage leading to weak streaks [2]. Early models [2–5] considered two lines of gold atoms and were supported by ion scattering spectroscopy (ISS) and reflection high-energy electron diffraction studies [5–7]. Scanning tunneling microscopy (STM) studies [8–10], however, appeared to contradict this, showing a more complicated structure with a feature shaped like a "Y" and an irregular decoration of protrusions. Other authors [9,11] have noted that there are too many STM features for all of them to be gold atoms, the coverage of which cannot be more than 0.5 ML [12]. [Reflection electron microscopy and STM studies indicate that the silicon content is significantly lower than in the Si(111)-(7 × 7) structure [13,14].] An x-ray diffraction study failed to give clean locations for the gold atoms and was fitted by a disordered structure with partial occupancies [15]. However, STM images, an x-ray standing wave analysis [16], and transmission electron diffraction patterns [17] do not show high disorder (aside from the phase slippage). The gold height from an x-ray standing wave study [16] and one ISS study [5] is within the first silicon double layer, while another ISS study [6] found the gold 0.7 Å above the outermost Si layer.

In this Letter we report the main details of this surface using a combination of high resolution electron microscopy (HREM), quantitative transmission electron diffraction (TED), and a direct phasing holographic inversion of the diffraction patterns. We show that all the available evidence fits a relatively simple model with gold atoms decorating a surface dislocation accommodating the intrinsic stress of the Si(111) surface.

Silicon (111) samples were prepared by a combination of *ex situ* thinning and *in situ* sputter-anneal cycles similar to previous work [18,19] within the side chamber of a UHV H9000 electron microscope [20]. Approximately half a ML of gold was deposited onto the surface and lightly electron beam annealed at about 550 °C (±50 °C). (Reannealing or cleaning the surface followed by repeated gold deposition and annealing to reproduce the structure were performed many times over a period of about one month.)

These samples were examined using the UHV H9000 by off-zone HREM [21] at 250 kV with the gold on the *top* surface and by quantitative TED [22] at 250 and 300 kV with the gold on the *bottom* surface. For the HREM images four different regions of a focal series of nine members were analyzed after digitization with an Optronics P1000 microdensitometer, all 36 images being 1024 × 1024 pixels in size. Noise reduction was performed using a modified parametric Wiener filter [23]. For the diffraction analysis two different orientations were used, one containing three domains while the other contained >90% of a single domain. (Data reduction and the calculation methodology was the same as in our previous work [18,19].) The first three data sets with 275, 268, and 310 beams each came from a region 18.8 nm thick tilted 45 mrad from the (111) zone. Only beams between 0.3 and 2.5 $Å^{-1}$ and those of the 5 × 1 sublattice were included, omitting the streak intensities (see Fig. 1). For the second region (with a tilt of 71 mrad and a thickness of 37.6 nm) 648 beams were collected. This data set was used in the final structure fitting but not in the holographic analysis since its errors were larger. We assumed a y-axis mirror in the half cell $0 < y < 0.5$ with a translational symmetry of (0.25,0.5); lifting the mirror symmetry had only a small effect on the final results.

Figure 1 shows a typical TED pattern, using a rectangular 10 × 2 unit cell, there are streaks for (h,k), $k = 2n + 1$ and sharp diffraction spots for $k = 2n$.

 0031-9007/95/75(11)/2172(4)$06.00

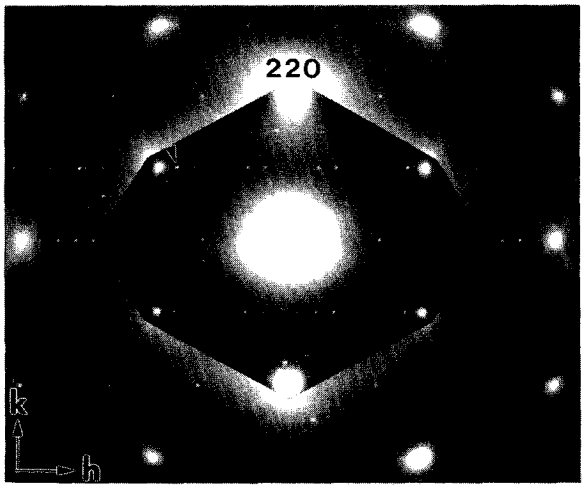

FIG. 1. TED pattern from a region with predominantly a single domain of the Si(111)-(5 × 2)-Au structure. This pattern was indexed in terms of a centered 10 × 2 unit cell; thus the arrowed strong surface beam is $(h, k) = (-13,2)$.

Figure 2 shows a typical near Schertzer defocus image where atoms appear black. Two lines of strong scattering features can be seen running along the [01] direction, which can be unconditionally identified as the gold atoms due to their strong scattering. There are also a number of not-well-resolved weaker features due to silicon atoms.

Although the HREM images clearly identify two lines of gold atoms, the structure has to be more complicated than this, as the weaker features in Fig. 2 show. In addition, the diffraction pattern is very inhomogeneous; for instance the (13,2) type is the strongest spot while (11,2) is quite weak.

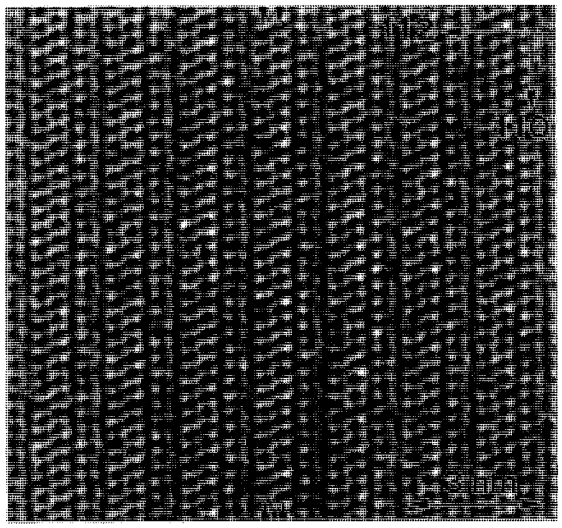

FIG. 2. Near Schertzer defocus, noise filtered, off-zone HREM image of the Si(111)-(5 × 2)-Au surface. Clearly visible are two (arrowed) rows of dark features which correspond to gold atoms.

One approach might be to use Fourier difference maps, but in practice we did not find these useful. A more powerful technique is based upon the heavy-atom method in x-ray diffraction [24]. Given an estimate for the wave $\Psi(\mathbf{u})$ generated by a χ^2 minimization with a given number of atoms, consider an additional wave $w(\mathbf{u})$ which minimizes:

$$R^2 = \langle [I(\mathbf{u}) - \alpha|\Psi(\mathbf{u}) + w(\mathbf{u})|^2]^2 \rangle, \qquad (1)$$

where in the simplest case $I(\mathbf{u})$ is the experimental diffraction intensities of a single domain and α the scaling constant determined by the χ^2 minimization. For the special case $R = 0$ Eq. (1) reduces to the general form of on-axis holography where both sidebands are invertible. This method, which we will refer to as "heavy-atom holography," exploits the interference between the known $\Psi(\mathbf{u})$ and an unknown $w(\mathbf{u})$ in the diffraction plane to determine the phase. (It should be noted that for electron diffraction in general $\Psi(\mathbf{u})$ has no special symmetry.) The Fourier transform of $w(\mathbf{u})$ is then an approximation of the residual wave, and by inspection candidate atomic locations can be determined. An example is shown in Figs. 3(a)–3(d). Additional sites are incorporated in a dynamical χ^2 TED minimization and the procedure repeated.

Although this formulation approaches a full solution, a more powerful method including measurement errors is required for the final steps. Extending Eq. (1) to many domains and including the dynamical diffraction effects before the bottom surface, one can write a more accurate χ^2 form:

$$\chi^2 = \sum \langle [I(\mathbf{u}) - \alpha|\Psi(\mathbf{u}) + w(\mathbf{u})^* T(\mathbf{u})|^2]^2 / \sigma(\mathbf{u})^2 \rangle, \qquad (2)$$

where $T(\mathbf{u})$ is the Fourier transform of the wave near the bottom of the sample just prior to the reconstructed layers (different for each domain) and $\sigma(\mathbf{u})$ the measurement errors. We determine $w(\mathbf{u})$ as above by minimizing χ^2. This form is better but does not include variations of the scaling constants α with $w(\mathbf{u})$. To handle these we find the smallest possible $w(\mathbf{u})$ (minimum-norm solution) that gives a χ^2 near one by minimizing $\langle w(\mathbf{u})^2 \rangle \exp(-\lambda\chi^2)$ with λ an adjustable constant typically in the range 0.1–0.5, and then we update the estimates of the scaling terms α periodically. An example is shown in Figs. 3(e) and 3(f) for determining the location of a Si adatom.

The final result is shown in Fig. 4, the x-y plane atom positions are listed in Table I, and the strongest intensities are listed in Table II. The χ^2 using all the experimental data was 3.6; using just the three holographic analysis domains it was 2.6. This χ^2 is for a structure with no subsurface relaxations. Including these is possible and for most surface structures necessary; however, here the experimental beam intensity errors in combination with the size and complexity of the surface unit cell make the usefulness of such a calculation doubtful.

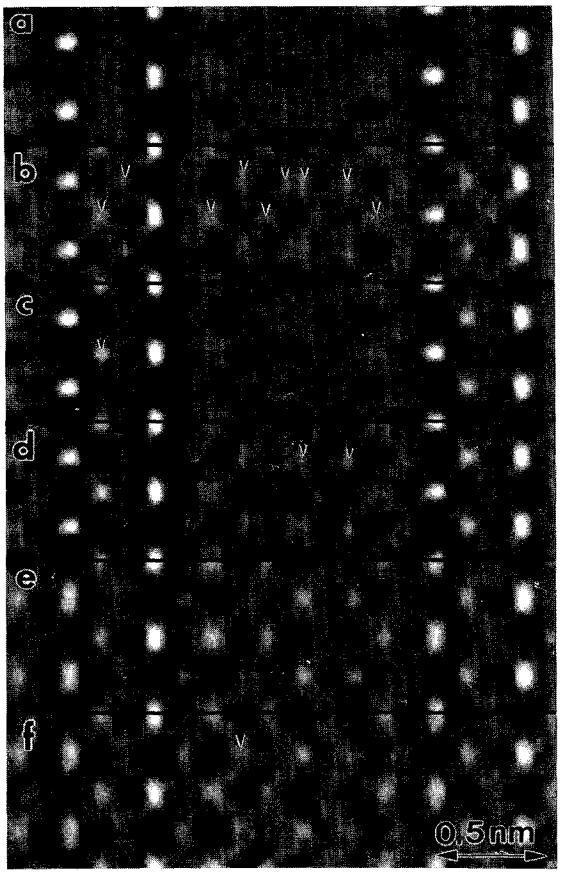

FIG. 3. Various stages of the Si(111)-(5 × 2)-Au structure solution for the silicon sites by heavy-atom holographic phasing. Starting in (a) with white gold atomic potential sites [$\Psi(\mathbf{u})$ in Eq. (1)] combined with the bulk wave exiting the sample, $\Psi(\mathbf{u}) + w(\mathbf{u})$ in (b) shows several possible silicon sites. Including the arrowed silicon site into the input wave in (c) the resulting wave (d) clearly shows two silicon sites while other potential sites in (b) are attenuated. In the later stages the use of Eq. (2) for the input wave (e) changes the shape of some sites but allows an adatom site to appear in the output, arrowed in (f).

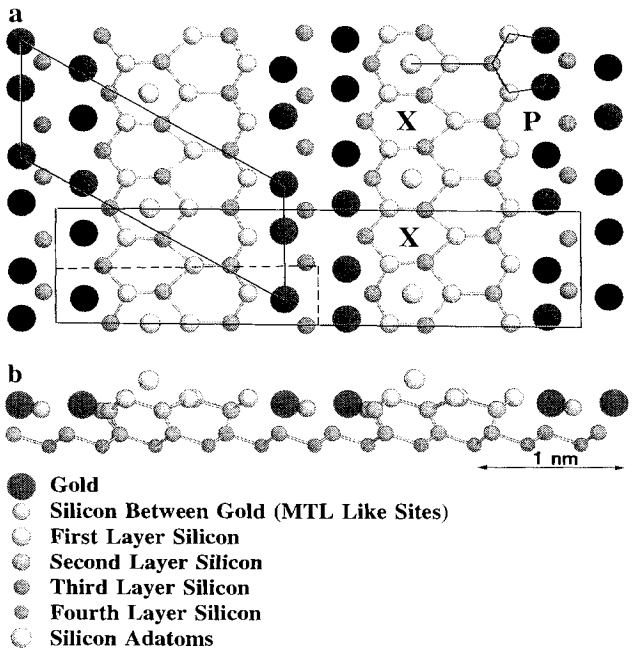

FIG. 4. (a) Top view of the Si(111)-(5 × 2)-Au atomic structure with the 5 × 2 primitive and the $c10 \times 2$ unit cells shown. The 5 × 1 subcell used in Table I is shown with dashes. Also shown is a "Y" like feature, an alternate set of Si adatoms sites (marked by "X"s), and the most probable type of site for the STM protrusions (marked "P"). (b) Side view of the structure. The gold atomic heights are taken from Ref. [16] and the silicon adatom heights are arbitrary. (No relaxations of the second silicon double layer were included in the calculation.) The surface silicon-silicon spacings expand and the surface dislocation accommodating the resultant stresses is decorated by the gold atoms.

Besides the subsurface relaxation, two additional ambiguities still exist. First, since we are only strongly sensitive to the atomic locations in the surface plane, the z (height) locations are inferred. Second, since the data is restricted to reflections from the 5 × 1 subcell (i.e., omitting the streak intensities), all the positions can be shifted by (0.5,0) without significantly changing the χ^2 value. The configuration that we have chosen best matches the HREM images.

The final structure appears to match all the available experimental evidence rather well. At the level of visual comparison, our Patterson function map is identical to that determined by x-ray diffraction. The gold atoms sit within the outermost silicon double layer slightly displaced from bulk lattice sites in agreement with the x-ray standing wave data and ISS. Silicon atoms appear between the two gold rows with gold-silicon spacings similar to the missing top layer structures proposed for the Si(111)-($\sqrt{3} \times \sqrt{3}$)$R30°$-Au surface [19]. If the silicon

TABLE I. Si(111)-(5 × 2)-Au atomic positions, Atoms refers to the total number of atoms of that site type in the $c(10 \times 2)$ unit cell, z direction layer positions are inferred (see text). Plane group $p1m1$ with a (0.5,±0.25) translational element for a $c(10 \times 2)$ surface unit cell: a = 33.252 Å, b = 7.679 Å.

Type	Site	Atoms	x [±0.003]	y [±0.013]	z [inf.]
Si	2c	2*	0.188	0.002	Layer 1
Si	2c	4	0.375	0.256	Layer 2
Si	1a	2	0.263	0.000	Layer 2
Si	1b	2	0.272	0.500	Layer 2
Si	2c	4	0.144	0.258	Layer 2
Au	2c	4	0.063	0.216	Layer 3
Au	2c	4	0.445	0.203	Layer 3
Si	2c	4	0.985	0.273	Layer 3
Si	2c	4	0.213	0.272	Layer 4
Si	1a	2	0.113	0.000	Layer 4
Si	1b	2	0.100	0.500	Layer 4
Si	1a	2	0.343	0.000	Layer 4
Si	1b	2	0.343	0.500	Layer 4

*Si adatom site with half occupancy.

TABLE II. Experimental and calculated diffraction beam intensities, experimental errors, and other error parameters for the strongest beams of Si(111)-(5 × 2)-Au.

Indices h	Indices k	Experim. Intensity	Calculat. Intensity	Absol. σ	Relat. σ (%)	Δ Intens. σ
0	0	1.00×10^{0}	1.00×10^{0}			
−13	−2	1.48×10^{-4}	1.37×10^{-4}	4.21×10^{-6}	2.84	2.66
−11	−2	1.70×10^{-5}	1.64×10^{-5}	1.43×10^{-6}	8.38	0.45
−3	−2	4.50×10^{-5}	4.93×10^{-5}	2.36×10^{-6}	5.24	−1.80
3	−2	4.50×10^{-5}	4.57×10^{-5}	2.13×10^{-6}	4.74	−0.30
11	−2	1.54×10^{-5}	1.77×10^{-5}	1.40×10^{-6}	9.06	−1.60
13	−2	1.39×10^{-4}	1.34×10^{-4}	3.22×10^{-6}	2.32	1.49
−18	0	2.39×10^{-5}	2.36×10^{-5}	2.02×10^{-6}	8.47	0.16
−16	0	2.17×10^{-5}	2.53×10^{-5}	2.51×10^{-6}	11.60	−1.46
−14	0	2.98×10^{-5}	2.51×10^{-5}	1.62×10^{-6}	5.42	2.92
14	0	3.08×10^{-5}	2.09×10^{-5}	1.75×10^{-6}	5.70	5.65
16	0	2.25×10^{-5}	2.07×10^{-5}	1.51×10^{-6}	6.72	1.21
18	0	3.05×10^{-5}	2.72×10^{-5}	2.48×10^{-6}	8.13	1.32
−13	2	1.38×10^{-4}	1.38×10^{-4}	3.37×10^{-6}	2.45	0.00
−11	2	2.03×10^{-5}	1.63×10^{-5}	2.56×10^{-6}	12.62	1.56
−3	2	4.42×10^{-5}	4.57×10^{-5}	2.11×10^{-6}	4.77	−0.68
3	2	4.29×10^{-5}	4.23×10^{-5}	2.04×10^{-6}	4.76	0.27
11	2	1.52×10^{-5}	1.83×10^{-5}	1.40×10^{-6}	9.19	−2.23
13	2	1.58×10^{-4}	1.33×10^{-4}	5.37×10^{-6}	3.41	4.62

adatom is interpreted as the bottom feature of the STM Y then the Y in Fig. 4(a) would be the only set of sites which could correspond to the STM features. From this we infer which set of silicon sites is the higher sites of the expanded silicon double layer. The reconstruction driving force appears to be expansion of the silicon surface spacings similar to Si(111)-(7 × 7), with the gold atoms segregating to the core of a surface dislocation that accommodates the strains [see Fig. 4(b)].

We should briefly comment about the "protrusions" seen approximately every other cell in some STM images [8–10] but not in another [25]. We tested the hypothesis of adding silicon adatoms with a partial occupancy of 0.4, the optimum location is the site marked "P" in Fig. 4(a), but the reduction in χ^2 was small. More significantly there is no evidence in our diffraction patterns for partially ordered defects. Defect ordering has been detected by Takahashi, Tanishiro, and Takayanagi [17], but only in samples heated at higher temperatures; the STM images which show protrusions [8–10] were prepared at higher temperatures than we used; no STM protrusions were observed in samples prepared at 500 °C [25].

This research was supported by the Air Force Office of Scientific Research under Grant No. F49620-92-J-0250.

[1] H. E. Bishop and J. C. Riviere, J. Phys. D **2**, 1635 (1969).
[2] H. Lipson and K. E. Singer, J. Phys. C **7**, 12 (1974).
[3] G. Lelay and J. P. Faurie, Surf. Sci. **69**, 295 (1977); G. Lelay, J. Cryst. Growth **54**, 551 (1981).
[4] Y. Tanishiro, K. Takayanagi, and K. Yagi, Report at the 36th Annual Meeting of the Physical Society of Japan, Hiroshima, 1981.
[5] Y. Yabuuchi, F. Shoji, K. Oura, and T. Hanawa, Surf. Sci. **131**, L411 (1983).
[6] J. H. Huang and R. S. Williams, Surf. Sci. **204**, 445 (1988).
[7] H. Daimon, C. Chung, S. Ino, and Y. Watanabe, Surf. Sci. **235**, 142 (1990).
[8] T. Hasagawa, K. Takata, S. Hosaka, and S. Hosoki, J. Vac. Sci. Technol. A **8**, 241 (1990).
[9] A. A. Baski, J. Nogami, and C. F. Quate, Phys. Rev. B **41**, 10 247 (1990).
[10] J. D. O'Mahony *et al.*, Surf. Sci. Lett. **277**, L57 (1992).
[11] J. D. O'Mahony *et al.*, Phys. Rev. B **49**, 2527 (1994).
[12] E. Bauer, Surf. Sci. Lett. **250**, L379 (1991).
[13] Y. Tanishiro and K. Takayanagi, Ultramicroscopy **31**, 20 (1989).
[14] T. Hasegawa, S. Hosaka, and S. Hosoki, Jpn. J. Appl. Phys. **31**, L1492 (1992).
[15] Ch. Schamper *et al.*, Phys. Rev. B **43**, 12 130 (1991).
[16] S. M. Durbin, L. E. Berman, B. W. Batterman, and J. M. Blakely, Phys. Rev. B **33**, 4402 (1986); L. E. Berman, B. W. Batterman, and J. M. Blakely, Phys. Rev. B **38**, 5397 (1988).
[17] S. Takahashi, Y. Tanishiro, and K. Takayanagi, Surf. Sci. **242**, 73 (1991).
[18] G. Jayaram, P. Xu, and L. D. Marks, Phys. Rev. Lett. **71**, 3489 (1993).
[19] R. Plass and L. D. Marks (to be published).
[20] L. D. Marks *et al.*, Ultramicroscopy **37**, 90 (1991); J. E. Bonevich and L. D. Marks, Microscopy **22**, 95 (1992).
[21] P. Xu and L. D. Marks, Ultramicroscopy **45**, 155 (1992).
[22] L. D. Marks, G. Jayaram, and R. Plass (to be published).
[23] H. C. Andrews and B. R. Hunt, *Digital Image Restoration* (Prentice-Hall, Englewood Cliffs, NJ, 1977), p. 150.
[24] J. M. Cowley, *Diffraction Physics* (North-Holland, Amsterdam, 1981), 2nd ed., p. 131.
[25] T. Hasegawa, S. Hosaka, and S. Hosoki, Jpn. J. Appl. Phys. **31**, 1492 (1992).

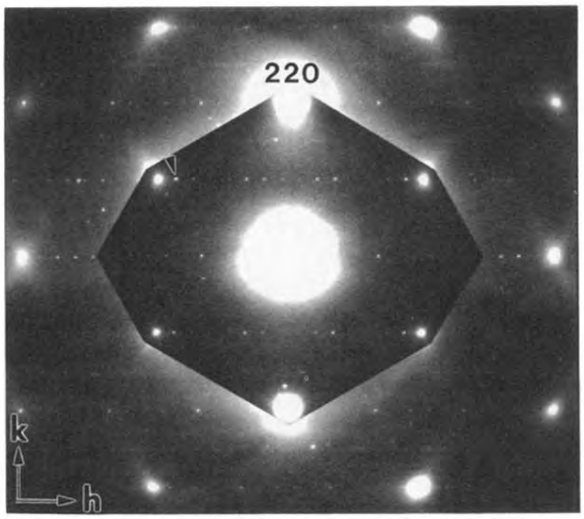

FIG. 1. TED pattern from a region with predominantly a single domain of the Si(111)-(5 × 2)-Au structure. This pattern was indexed in terms of a centered 10 × 2 unit cell; thus the arrowed strong surface beam is $(h, k) = (-13,2)$.

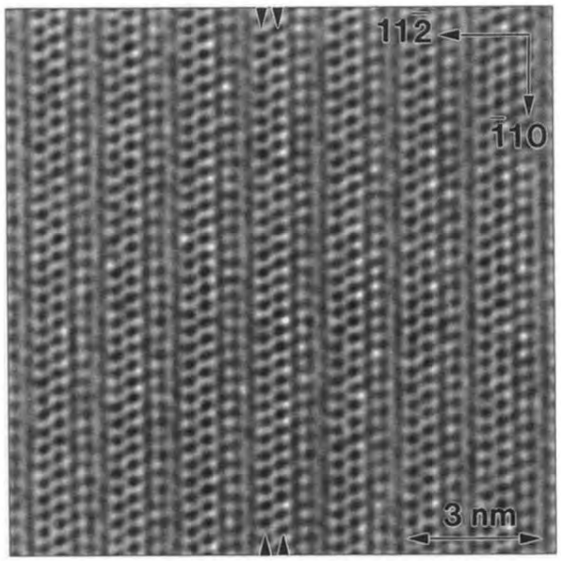

FIG. 2. Near Schertzer defocus, noise filtered, off-zone HREM image of the Si(111)-(5 × 2)-Au surface. Clearly visible are two (arrowed) rows of dark features which correspond to gold atoms.

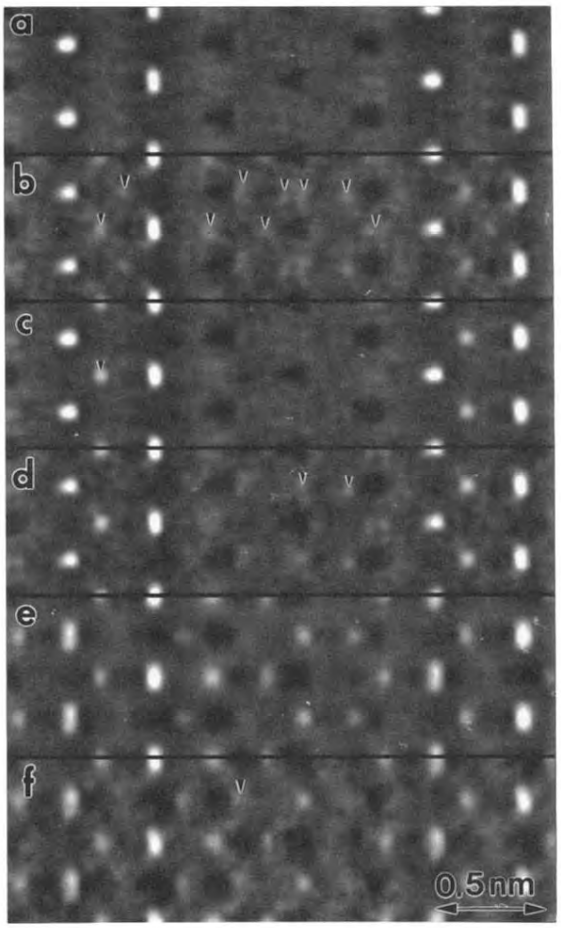

FIG. 3. Various stages of the Si(111)-(5 × 2)-Au structure solution for the silicon sites by heavy-atom holographic phasing. Starting in (a) with white gold atomic potential sites [$\Psi(\mathbf{u})$ in Eq. (1)] combined with the bulk wave exiting the sample, $\Psi(\mathbf{u}) + w(\mathbf{u})$ in (b) shows several possible silicon sites. Including the arrowed silicon site into the input wave in (c) the resulting wave (d) clearly shows two silicon sites while other potential sites in (b) are attenuated. In the later stages the use of Eq. (2) for the input wave (e) changes the shape of some sites but allows an adatom site to appear in the output, arrowed in (f).

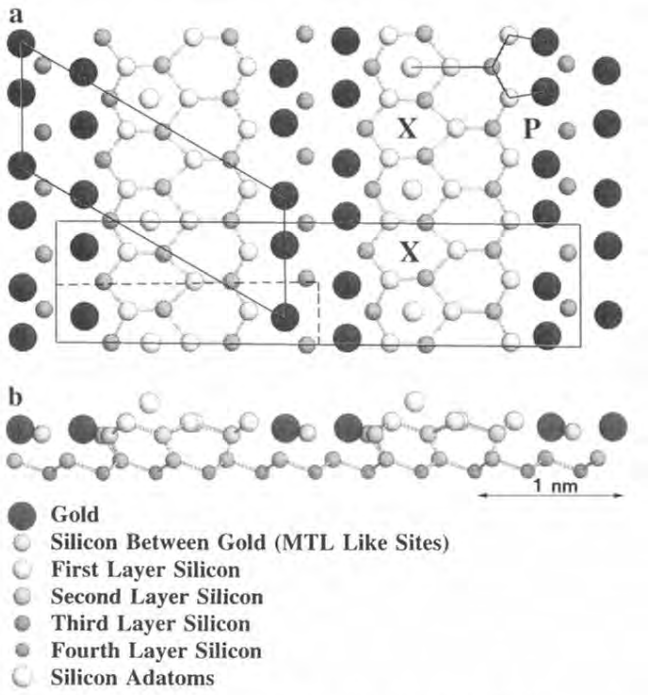

FIG. 4. (a) Top view of the Si(111)-(5 × 2)-Au atomic structure with the 5 × 2 primitive and the $c10 \times 2$ unit cells shown. The 5 × 1 subcell used in Table I is shown with dashes. Also shown is a "Y" like feature, an alternate set of Si adatoms sites (marked by "X"s), and the most probable type of site for the STM protrusions (marked "P"). (b) Side view of the structure. The gold atomic heights are taken from Ref. [16] and the silicon adatom heights are arbitrary. (No relaxations of the second silicon double layer were included in the calculation.) The surface silicon-silicon spacings expand and the surface dislocation accommodating the resultant stresses is decorated by the gold atoms.